water

MDPI

Article

Temperature and Secchi Disk Depth Increase More Rapidly in the Subpolar Bering/Okhotsk Seas Than in the Subtropical South China Sea

Chen-Tung (Arthur) Chen [1,*], Shujie Yu [2], Ting-Hsuan Huang [3], Yan Bai [2], Xianqiang He [2] and Hon-Kit Lui [1]

[1] Department of Oceanography, National Sun Yat-Sen University, Kaohsiung 804, Taiwan
[2] State Key Laboratory of Satellite Ocean Environment Dynamics, Second Institute of Oceanography, Ministry of Natural Resources, Hangzhou 310012, China
[3] Taiwan Ocean Research Institute, National Applied Research Laboratories, Kaohsiung 801, Taiwan
* Correspondence: ctchen@mail.nsysu.edu.tw; Tel.: +886-7-525-5136

Abstract: Like other high-latitude seas, the subpolar Bering and Okhotsk Seas in the northernmost Pacific Ocean changed rapidly from 1998 to 2018. The sea surface temperature (SST) increased by 0.62 and 0.41 °C/decade, respectively, much higher than the global rate of 0.108 °C/decade from 2000 until 2015. Despite this rapid warming, the chlorophyll content did not change significantly in the Bering Sea but increased by 0.047 μg/L/decade in the Okhotsk Sea. The Secchi disk depth (SDD) increased by 0.43 and 0.46 m/decade, respectively. Similar to other warm bodies of water, the SST of the subtropical/tropical South China Sea (SCS) also began rising, by 0.089 °C/decade, albeit more slowly than the global average. The chlorophyll content increased at 0.15 μg/L/decade from 1998 to 2006 but decreased by 0.11 μg/L/decade between 2007 and 2018. The SDD increased by 0.29 m/decade between 1998 and 2018. Although the SDD increased in all three seas, the chlorophyll concentration was maximum around 2006–2009, reflecting different phytoplankton responses to seawater warming.

Keywords: Bering Sea; Okhotsk Sea; South China Sea; sea surface temperature; chlorophyll concentration; Secchi disk depth; temporal trends; global warming; carbon sequestration

Citation: Chen, C.-T.; Yu, S.; Huang, T.-H.; Bai, Y.; He, X.; Lui, H.-K. Temperature and Secchi Disk Depth Increase More Rapidly in the Subpolar Bering/Okhotsk Seas Than in the Subtropical South China Sea. *Water* **2023**, *15*, 98. https://doi.org/10.3390/w15010098

Academic Editor: Guangyi Wang

Received: 5 November 2022
Revised: 5 December 2022
Accepted: 14 December 2022
Published: 28 December 2022

1. Introduction

Marginal seas of the Asia Pacific are among the most productive areas in the world and support the livelihood of hundreds of millions of people. Solar energy, nutrient concentrations, SST, seawater turbidity (represented by the SDD), and primary productivity (characterized by the chlorophyll concentration), among other things, affect fisheries production, which is a significant source of protein in the region. The SST and chlorophyll concentration are also two important factors affecting the air–sea exchanges of oxygen and CO_2. Here, we use readily available satellite data to investigate the trends in SST, chlorophyll content, and SDD in the subpolar Bering/Okhotsk Seas and compare these trends with those in the subtropical South China Sea. Other than showing the subpolar vs. subtropical contrasts, our results are compared with findings in other marginal seas and the open oceans.

In the era of global warming, the SST has been rising everywhere. The consequent increase in the water column's stratification weakens the upward pumping of nutrients from the nutrient-rich subsurface layer. Thus, biological productivity declines in the global open oceans [1–3]. However, marginal seas may act differently because of the increasing anthropogenic nutrient input from rivers, submarine groundwater discharge, sewage outflows, or land-sourced aerosols [4–6].

Compared to the well-studied but smaller marginal seas such as the East China Sea (ECS), the three largest marginal seas in the Pacific Ocean—the Bering, Okhotsk Sea, and the

South China Seas—have received less attention. The subpolar Bering Sea (Figure 1) is the third-largest marginal sea globally after the South China Sea (SCS) and the Mediterranean Sea [7]. Like most marginal seas, the Bering Sea is more eutrophic than the open oceans and has one of the world's highest productivities [8].

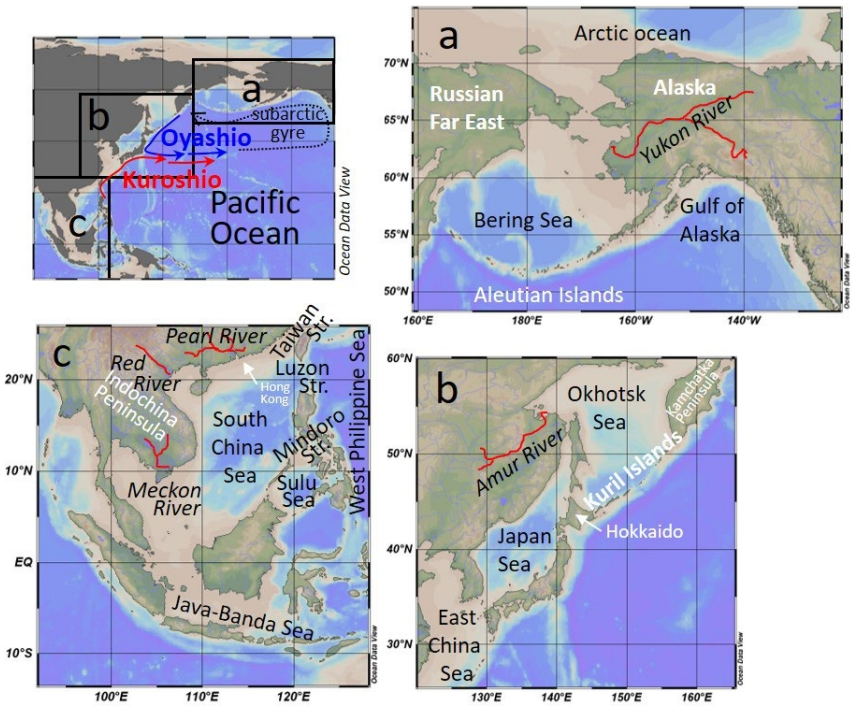

Figure 1. Maps of the (**a**) Bering, (**b**) Okhotsk, and (**c**) South China Seas (R. Schlitzer, Ocean Data View, http://odv.awi.de, 2018; accessed on 15 April 2019).

The Okhotsk Sea (Figure 1b) is the sixth-largest marginal sea globally and the third-largest in the North Pacific. Although geographically this sea is located at temperate latitudes, it has many characteristics of a polar ocean. The subtropical SCS (Figure 1c) is the world's most immense marginal sea and connects the Pacific and Indian oceans [9]. The West Philippine Sea (WPS) is the primary source of water for the SCS.

Numerous works report that increasing SST may reduce primary productivity (PP) and ocean biomass. In response to warming, there is a poleward migration of tropical and sub-tropical biota between estuaries [10]. However, different areas of the highly variable marginal seas may respond to global warming on various time scales [11]. The SST in all three seas has increased [12–16]. This paper concerns recent changes between 1998 and 2018.

Climate change has affected all marginal seas. For example, in the Okhotsk Sea, the extent of sea ice has decreased while the shelf water's salinity has been reduced [17]. More open waters in the winter may facilitate the air–sea exchange of oxygen and the uptake of more anthropogenic CO_2. However, DO concentrations in the Bering, and Okhotsk Seas have generally declined over the last five decades, although it has increased in the SCS [18–21]. Locally, the DO concentration has fallen because of eutrophication, such as in the bottom waters offshore Hong Kong [6].

Like the two seas reported above, the SCS surface water salinity has also been falling [22]. This is in line with the notion that seas with relatively low salinities, such as most marginal seas, are falling in salinity. On the other hand, more saline regions have increased salinity [23]. SCS water's freshening is due to a drop in salty Kuroshio water intrusion between 1993 and 2012 [22,24,25]. However, Lui et al. [26] reported that the Luzon Strait had experienced increased Kuroshio intrusion since 2012. These complicated processes affect SCS's biogeochemistry. Nutrient and inorganic carbonate concentrations and water transport from the SCS to the ECS are rising overall. This rise is related to an

abnormal change in sea surface height [27]. These signals correlate with the PDO and provide overall patterns of environmental changes in the three seas studied.

These three seas have had a fall in pH due to the penetration of excess CO_2 from the atmosphere [6,28,29]. Similar to what happens in the open oceans (e.g., Bindoff et al., 2019 [1]; IPCC, 2022 [3]), values of many biophysical metrics have also changed in marginal seas. Yet there have been very few reports of quantitative temporal trends exhibited by these seas in contrasting environments. What follows investigates temporal changes in SST, chlorophyll content, and Secchi Disk Depth (SDD) in these three seas between 1998 and 2018 based on satellite data, and provides a mini-review of synthesized results of long-term changes by incorporating recent literature data. Results are compared with what was found in other marginal seas and in the open ocean.

2. Sea Surface Temperature

Changes in SST between 1998 and 2018 are based on the Advanced Very High-Resolution Radiometer satellite data with a spatial resolution of 0.25°. This data can be obtained from NOAA's National Centers for Environmental Information (https://data.nodc.noaa.gov/ghrsst/L4/GLOB/NCEI/AVHRR_OI/; accessed in 15 April 2019). Pixels were removed when the number of available data was less than half of the total data, most likely due to cloud coverage. In some areas, the SST may represent ice surface temperature. Chen et al. [14,15] provided the details. The climatological SST was lowest, below 3 °C, on the continental shelf in the NE Bering Sea. The SST was slightly higher in the deep basin and jumped to 7 °C south of the Aleutian Islands. A sizeable seasonal variation occured from an average temperature of 1 °C in February to 10 °C in August (Figure 2a). The highest SST increase occured in the western basin, reaching 0.6–0.8 °C/decade from 1998 until 2018 (Figure 3a), similar to other high-latitude seas [30,31]. The overall average SST increased by 0.62 °C/decade (p = 0.06) based on the linear fit (Table 1). The cubic polynomial fit gave the same p-value, but the end effect was significant (Figure 3a). Of note is that because the data record is short, a few years of data can change the trend tremendously.

Table 1. Temporal changing rate and statistics of SST, Chl, and SDD during 1998–2018.

		Mean	Changing Rate (%/yr)	Changing Rate (/Decade)	p Value
Bering Sea	SST	4.34 °C	-	0.62 °C	0.06
	Chl	1.43 µg/L	−0.05	−0.007 µg/L	0.92
	SDD	13.41 m	0.32	0.432 m	0.37
Okhotsk Sea	SST	4.35 °C	-	0.408 °C	0.38
	Chl	1.57 µg/L	0.30	0.047 µg/L	0.56
	SDD	12.67 m	0.36	0.457 m	0.30
South China Sea	SST	27.97 °C	-	0.089 °C	0.52
	Chl	0.44 µg/L	−0.02	−0.001 µg/L	0.91
	SDD	30.03 m	0.10	0.289 m	0.36

The SST increase is comparable with Belkin [32] 's 1.1 °C/decade warming between 1982 and 2006 in the eastern Bering Sea. By comparison, the global SST increased by less than 0.15 °C/decade from 2000 to 2015 [31] and is projected to increase by 2.2 °C by the end of the century, based on the RCP2.6 scenario [33]. The Arctic, including the Bering Sea, has been projected to become warmer and ice-free in summer by 2050 [34]. Increasing SST promotes phytoplankton growth in regions where the temperature is generally too low for optimal phytoplankton growth, as discussed further in the next section.

The annual mean SST was below 7 °C in the Okhotsk Sea, except in the south [15]. Like the Bering Sea, the Okhotsk Sea's SST also exhibited a sizeable seasonal variation; below 0 °C in winter but reaching 13 °C in summer (Figure 2b). Coastal waters of the Kamchatka Peninsula experienced a substantial rise of 0.5–0.6 °C/decade (Figure 3b), resulting in

recent enhanced phytoplankton growth. Overall, the temporal SST change from 1998 until 2018 of 0.41 °C/decade over the entire Okhotsk Sea was statistically insignificant (p = 0.38; Figure 3b and Table 1), although the central and eastern regions of the sea warmed (Figure 3b). He et al. [31] saw a similar increase of 0.5 °C/decade from 1998 to 2010, but Belkin [32] found a much lower rate of 0.13 °C/decade between 1982 and 2006. Different satellite data sources and periods might have contributed to the difference between these SST-increasing rates. A more extended time series generally yields a minor change because of temporal smoothing.

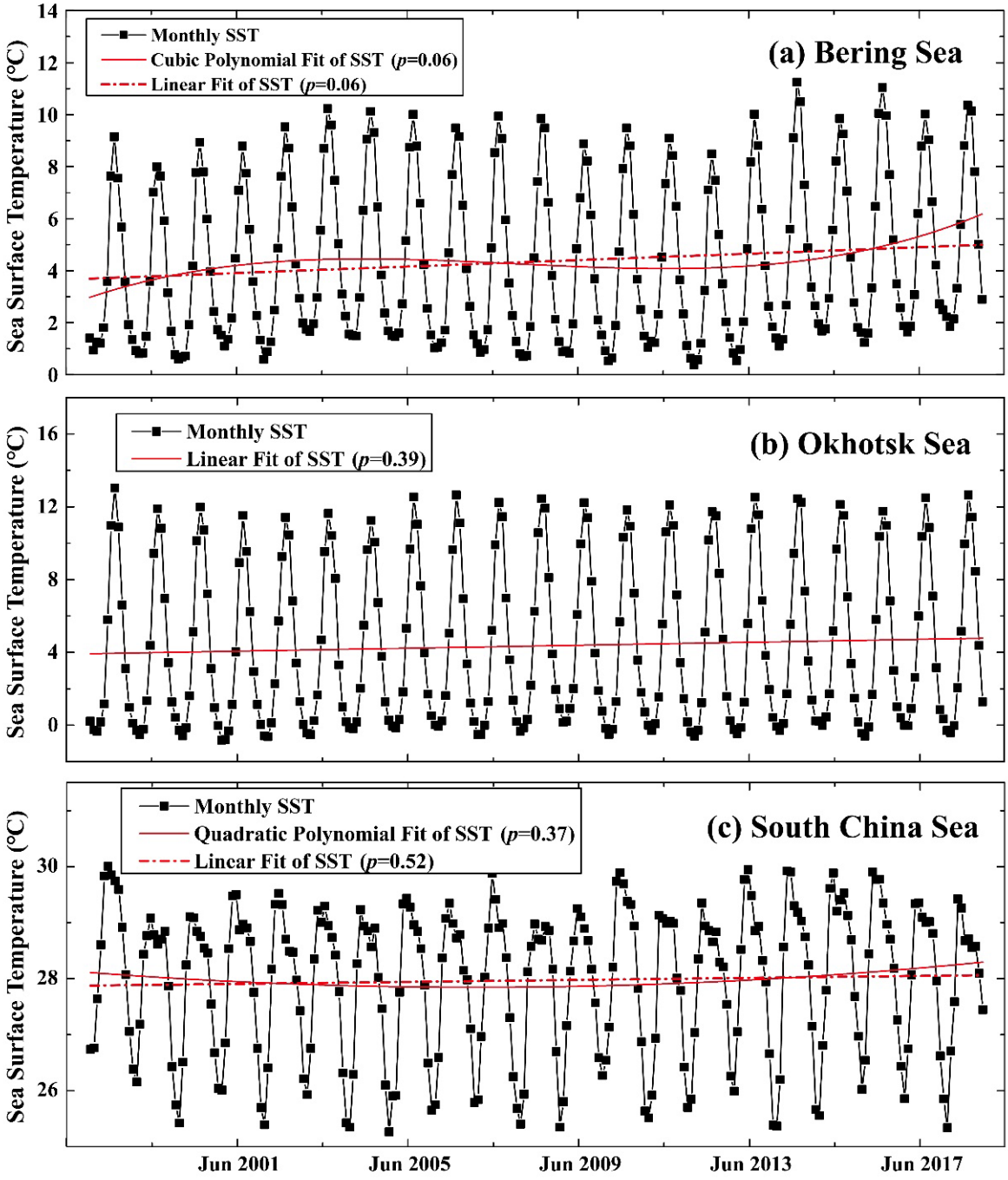

Figure 2. SST time series in the (**a**) Bering, (**b**) Okhotsk, and (**c**) South China Seas during 1998–2018.

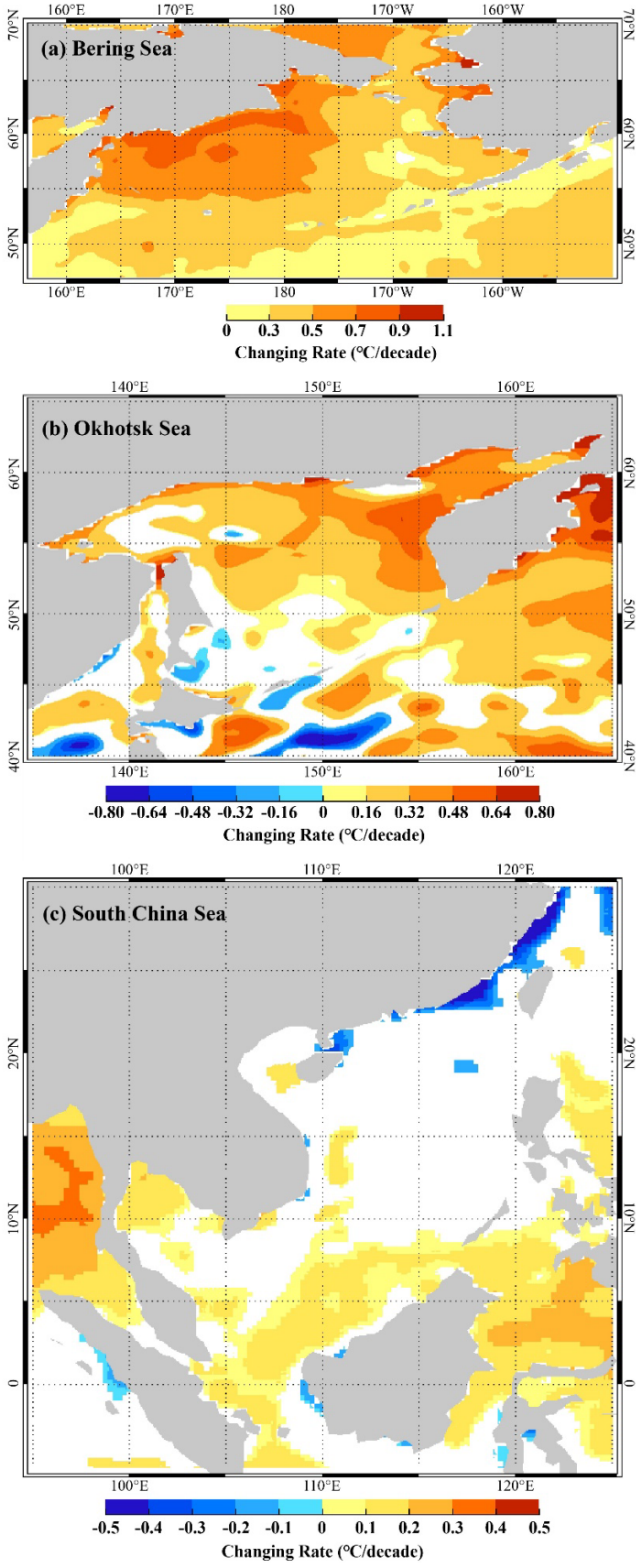

Figure 3. SST trends in the (**a**) Bering, (**b**) Okhotsk, and (**c**) South China Seas during 1998–2018 (bright colors show pixels with $p < 0.1$).

Unlike high-latitude seas, the climatological SST of the SCS generally tops 26 °C, except in China's southeast coastal region [16], where the cold Chinese coastal waters flow southward when the NE monsoon prevails. This coastal water transports nutrients from the ECS to the SCS [35–38]. Figure 2c shows SCS's SST. In contrast to the high-latitude seas which have a considerable seasonal SST variation, SCS's SST varied only between 25 °C and 30 °C. Geographically, offshore SE China, with the lowest SST, had a declining SST. Yet the warmest areas in the southern SCS experienced increases (Figure 3c). In the mid and south SCS, the SST increased significantly at 0.1–0.2 °C/decade from 1998–2018, putting pressure on the growth of corals. Periodically SST drops due to internal waves or typhoons lessen the thermal stress [39,40], but these events were not apparent in the long-term satellite records. It is important to point out that the SST fell broadly in coastal waters off SE China and in the Taiwan Strait, where the chlorophyll content increased significantly (Figure 4c; [27]). This cooling may suggest increased coastal upwelling or enhanced southward transport of the ECS water in winter due to stronger winds, which would have increased surface nutrient supply, favoring phytoplankton growth.

In addition, the high-latitude seas generally saw an increasing SST from 1998 to 2018 (0.62 °C/decade and 0.41 °C/decade for the Bering Sea and the Okhotsk Sea, respectively). However, there was only an insignificant linear increase of 0.089 °C/decade in the SCS (p = 0.52; Figure 2c and Table 1). The SST's quadratic polynomial fit had a slightly lower p-value of 0.37 (better correlation; Figure 2c) than the linear fit. There was a better quadratic fit because the SST fell initially after the strong El Niño year of 1997/98 when widespread warming occurred [41] and increased subsequently. However, the surface mixing layer became shallower from 1992–2000 [42], because of rising SST, especially during 1997/98. Globally, the SST increase was also uneven, with a slower rate in the tropical region [43].

Many reports have discussed SCS's temporal SST variations, but the results depend on the period covered. He et al. [31] found little change between 1998 and 2010. Giuliani et al. [44] detected an increase of 0.28 °C/decade from 1960 to 2011, similar to that obtained by Bai et al. [11] (around 0.3 °C/decade from 2003 to 2014) in low-latitude Eurasian marginal seas; including the SCS, the Java-Banda Sea, the Bay of Bengal, and the Arabian Sea.

A comparison of other marginal seas around the globe reveals that the North Sea had warmed more slowly (0.13 °C/decade) than the roughly 0.5 °C/decade, of the Bering and Okhotsk Seas, despite their similar latitudes. The Bering and Okhotsk Seas are semi-enclosed, and their seemingly high warming rate between 1998 and 2018 was only moderate. Bai et al. [11] reported that enclosed marginal seas warmed more than open marginal seas based on the study of 12 seas around the Eurasian continent from 2003 to 2014; they did not cover the Bering and Okhotsk Seas.

The Black Sea had the fastest warming (0.19 °C/decade), followed by the Baltic and the Mediterranean Seas (0.1 °C/decade). The Sea of Japan, the ECS, and the Persian Gulf also showed rapid warming (0.9 °C/decade). The low-latitude SCS, the Bay of Bengal, the Java-Banda, Arabian, and the Red Seas exhibited slower warming (~0.3 °C/decade). Bai et al. [11] covered a period of 12 years without including the strong El Niño year of 1997–1998; the present study considers 21 years (1998–2018), possibly yielding a lower rate of change.

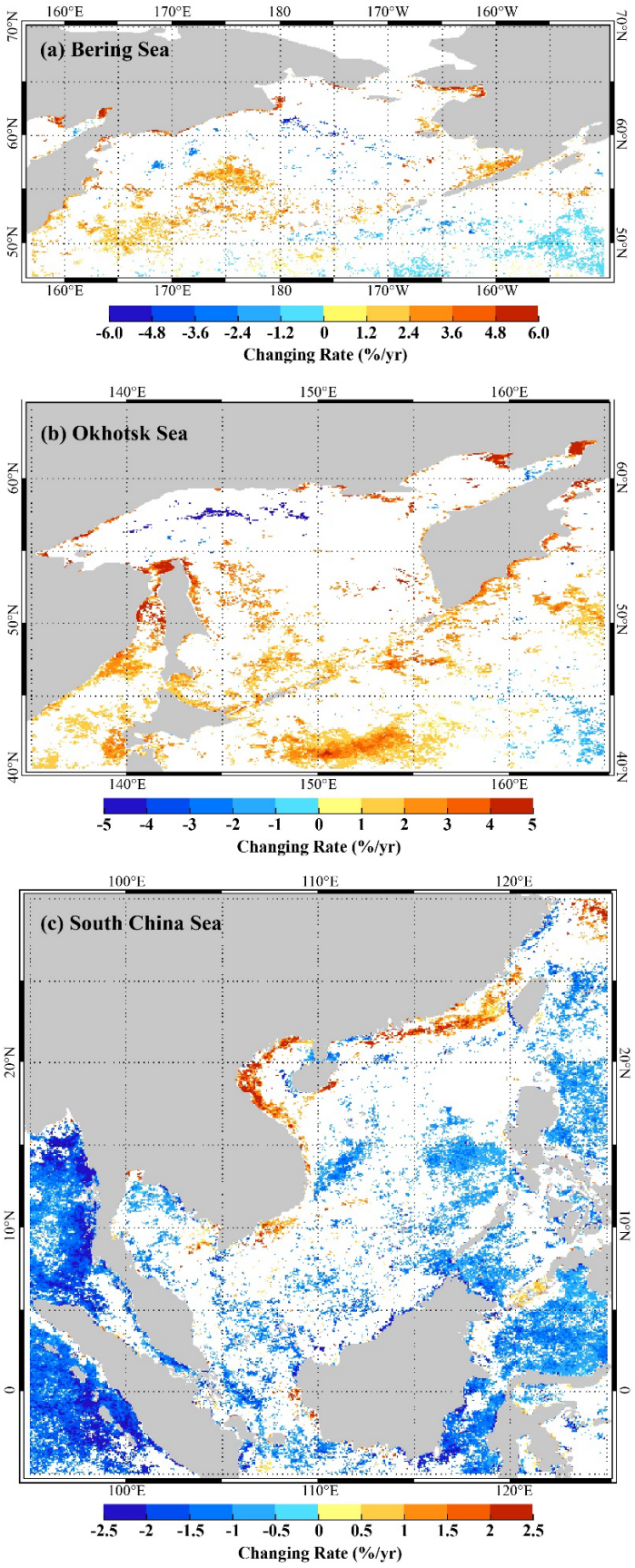

Figure 4. Chlorophyll trends in the (**a**) Bering, (**b**) Okhotsk, and (**c**) South China Seas during 1998–2018 (bright colors show pixels with $p < 0.1$).

3. Chlorophyll Concentration

Earlier, we obtained a time series of chlorophyll concentration in the three studied seas from the Ocean Color project of the European Space Agency (ESA) Climate Change Initiative [14–16]. Monthly L3S chlorophyll concentrations with a spatial resolution of 4 km were used (http://www.esa-oceancolour-cci.org; accessed in 15 April 2019). Pixels were removed in turbid waters with reflectance at 555 nm larger than 0.1/sr. To diminish the effects of clouds and sea ice, we have used the monthly composited products rather than the daily or 8-day composited products as they exhibit high spatial-temporal variability. As a result of the terrestrial outflow of nutrients, entrainment by river plumes, coastal upwelling, and wind and tidal mixing, the coastal regions, especially bays and those parts within the plumes offshore of the Yukon and Amur Rivers, exhibit higher chlorophyll contents than deeper waters [14–16,36,45–47]. For example, chlorophyll concentrations reached 10 μg/L in the bay off the Yukon River in western Alaska, partly reflecting the thawing of permafrost in the river basin [48]. These coastal concentration seemed to be on the rise (Figure 4a,b). The chlorophyll concentration fell between 1 and 3 μg/L on the continental shelf and off Eastern Siberia compared with values lower than 1 μg/L in the deep basin [14]. The chlorophyll content had a considerable seasonal variability (Figure 5a,b), typically reaching a maximum in late spring and a minimum in winter, similar to that observed in other high-latitude seas, possibly a combined effect of limited solar radiation and sea ice's shielding effect in winter.

The chlorophyll content in the Bering and Okhotsk Seas shows an overall increasing trend of 0.35 and 0.38 μg/L/decade, respectively, between 1998 and 2008 (p = 0.04 and 0.06, respectively; Figure 5a,b and Table 2), similar to what He et al. [31] reported for 1997–2010. However, between 2009 and 2018, the chlorophyll concentration decreased by 0.31 μg/L/decade in both seas (p = 0.11 and 0.21, respectively; Figure 5a,b, and Table 2). Overall, between 1998 and 2018, the chlorophyll concentration remained steady in the Bering Sea and increased slightly by 0.047 μg/L/decade in the Okhotsk Sea (p = 0.56; Figure 5b and Table 2). However, there was a significant increase in the southern Bering Sea (4–5%/yr) in that period, although the change was not apparent on the continental shelf (Figure 4a). Patches of these two seas showed a decreasing trend (blue in Figure 4a,b)

Table 2. Changing rate and statistical information of Chl during different periods.

	Time Scale		Mean Chl (μg/L)	Changing Rate (%/yr)	Changing Rate (μg/L/Decade)	p Value
Bering Sea	Phase 1	1998–2008	1.44	2.41	0.347	0.04
	Phase 2	2009–2018	1.41	−2.22	−0.313	0.11
		1998–2018	1.43	−0.05	−0.007	0.92
Okhotsk Sea	Phase 1	1998–2008	1.55	2.46	0.383	0.06
	Phase 2	2009–2018	1.59	−1.93	−0.307	0.21
		1998–2018	1.57	0.30	0.047	0.56
South China Sea	Phase 1	1998–2006	0.43	3.49	0.151	<0.005
	Phase 2	2007–2018	0.44	−2.52	−0.112	<0.005
		1998–2018	0.44	−0.02	−0.001	0.91

Significant increases occurred in the Okhotsk Sea, except in northwestern regions where sporadic declines occurred (Figure 4b). The most significant rise of 4–5%/yr happened in the central basin and in the northeastern bay. These findings are consistent with Bai et al.'s [11] finding that high-latitude Eurasian marginal seas displayed higher chlorophyll content between 2003 and 2014. The Baltic, Japan, and East China Seas showed the largest increase of 1.92%/yr, 1%/yr, and 1%/yr, respectively).

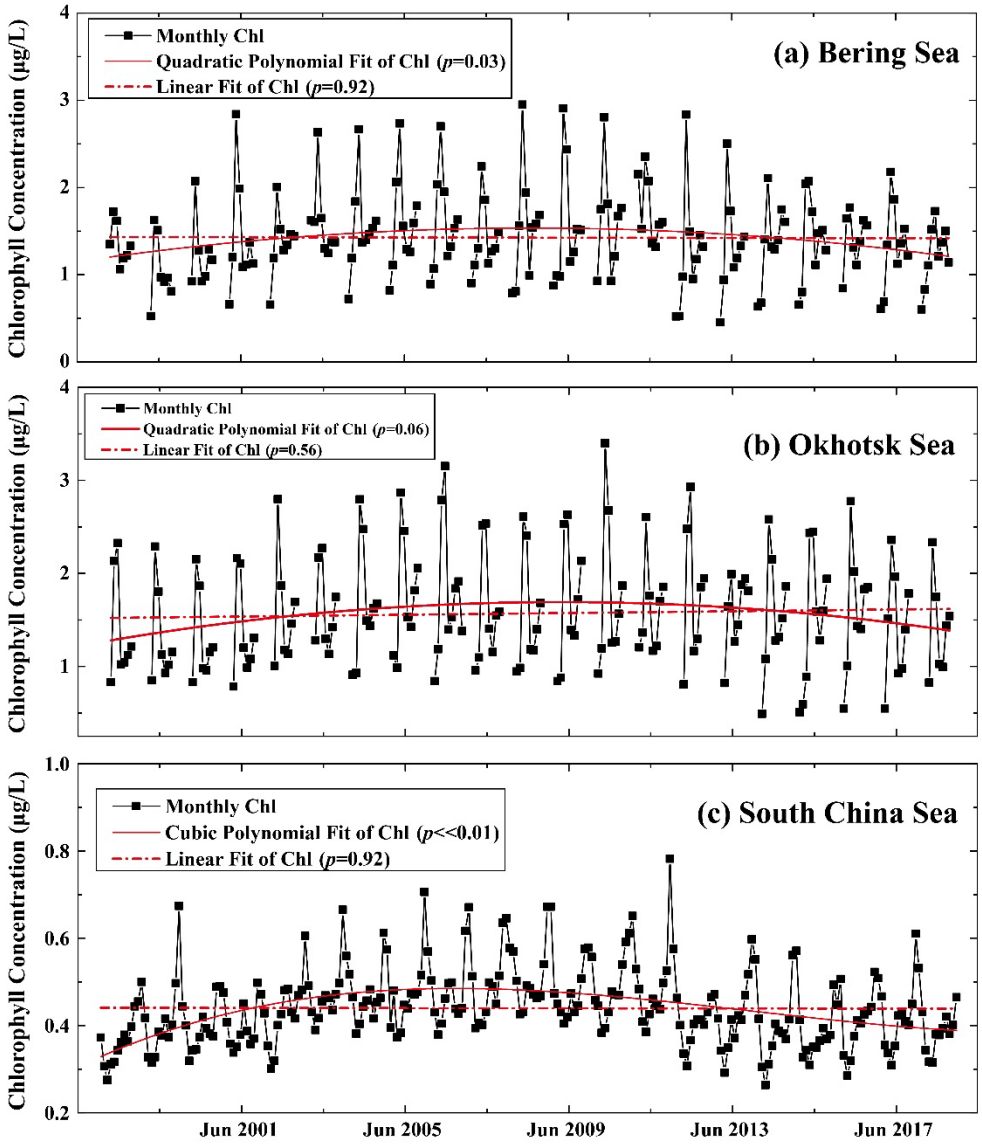

Figure 5. Time series of chlorophyll concentration in the (**a**) Bering, (**b**) Okhotsk, and (**c**) South China Seas during 1998–2018.

A higher SST generally results in a more stable water column, inhibiting nutrient supply from nutrient-rich deep layers to the oligotrophic surface euphotic layer, thereby lowering PP and chlorophyll content. Siegel et al. [49] indeed reported that in the world's warm regions with an annual-mean SST above 15 °C, the chlorophyll value decreased significantly (0.18%/yr) from 1998 to 2011. Interestingly, they detected that the chlorophyll increased significantly (0.83%/yr) in the open seas of the high-latitude Southern Hemisphere, with an annual-mean SST below 15 °C. However, they reported no change in the high latitude Northern Hemisphere's cold water regime, where the SST was less than 15 °C. Giesbrecht [50] also identified little variation in the Bering Sea between 2006 and 2016.

Thomas et al. [51] stated that phytoplankton's optimal growth temperature typically exceeds the local ambient SST at mid and high latitudes. As a result, any SST increase in those regions makes the habitat come closer to the optimal temperature for certain phytoplankton species, possibly increasing their growth rate and thereby increasing the chlorophyll content. Furthermore, increasing global SST may also cause poleward shifts of phytoplankton communities, thus increasing phytoplankton biomass and PP at higher latitudes. As shown above, the Bering and Okhotsk Seas have warmed.

Of note is that warming reduces oxygen solubility. Higher temperature also increases metabolic rates, enhancing organic carbon and oxygen consumption [52]. However, an increase in chlorophyll concentration accelerates oxygen production. The outcome of these opposing effects is that the DO in most of the Bering and Okhotsk Seas has fallen since 1960 [18]. It is concluded that the increase in SST has a more significant role than the increase in chlorophyll content in reducing these seas' DO.

From 1998–2018, chlorophyll concentrations significantly increased on the northern continental shelf of the SCS and off the Indochina Peninsula, in line with recent findings of Yu et al. [53] based on satellite data from 2002 to 2017. The chlorophyll concentration in the Taiwan Strait and the north SCS generally increased by 2.5%/yr between 1998–2018 (Figure 4c). Increased anthropogenic nutrient inputs or enhanced coastal upwelling have likely contributed to increasing chlorophyll. Patches of declining chlorophyll concentration formed sporadically in the central SCS basin and, inside those patches, the chlorophyll content fell by 1–1.5%/yr (Figure 4c). There was little variation from 1998 to 2018 (Figure 5c). Quadratic polynomial fitting reveals that the chlorophyll level initially increased and then decreased in those years. Figure 5c depicts a rise in chlorophyll concentration from 1998 to 2006 (0.15 μg/L/decade) and a decrease (−0.11 μg/L/decade) from 2007 to 2018, consistent with the two-phase changes observed in the Bering and Okhotsk Seas. However, the chlorophyll concentration has been falling in the Kuroshio region to the east of the SCS [54]. He et al. [31] detected no apparent change in the SCS between 1997 and 2010, whereas Palacz et al. [55] reported an increase of 0.04 μg/L (9%) over the same period. Li et al. [56] reported a rise from 2000 to 2014, although QP Li, the lead author of that paper, claimed no clear trend (personal communication, 12 January 2018). Bai et al. [11] reported a minimal increase (<0.001 μg/L/yr) from 2003 to 2014, in contrast to decreases in other tropical marginal seas, including the Arabian, Java-Banda, and the Red Seas, the Persian Gulf, and the Bay of Bengal.

As mentioned above, SCS's chlorophyll concentration (Figure 5c) increased between 1998 and 2008 but fell after that. The year 1998 was a strong El Niño year when the SST was high, resulting in lower surface-water density and a more stable water column. Consequently, there was less vertical mixing than in other years, and smaller amounts of nutrients were pumped to the surface layer. The result was lower PP and chlorophyll content. Gregg and Rousseux [57] pointed out that it is an unfortunate artifact that the strong El Nino coincided with the launch of the modern satellite ocean color sensor. The so-called endpoint effect is a matter of concern.

Furthermore, it is difficult to predict future changes as riverine nutrient input would increase while the warmer surface layers would inhibit the mixing of generally nutrient-depleted surface layers with nutrient-rich deeper waters. In addition, marine biota's physiological responses to nutrient concentrations and factors such as those caused by eddies, typhoons, and aerosol deposition may also change [58]. As in most other oceans, oxygen concentrations have been falling in the SCS basin. However, the oxygen concentration increased off SE China and the Indochina Peninsula during the study period [19], possibly due to the decrease in SST (higher oxygen solubility) and increased PP (more oxygen production), as revealed by the increasing chlorophyll content there (Figure 4c).

Interestingly, sediment traps in the basin of the SCS reveal that the content of particulate organic carbon and nitrogen (POC, PON) in the falling particles increased. Despite this, the POC/PON ratio still decreased, likely due to increasing anthropogenic nutrient inputs, which have caused the chlorophyll content in Hong Kong waters to rise since 1990 (Figure 4c; [26]). However, the DO concentration in the bottom layer declined from 2008 to 2018 due to increasing phytoplankton decomposition [26]. Intuitively, this latter finding seems inconsistent with the observed fall in chlorophyll content. The result is intriguing because the lower net PP corresponds to higher export efficiency in the SCS [59], where PP correlates positively with chlorophyll [60], so the falling chlorophyll content between 2007 and 2018 (Table 2) reflects a fall in net PP. Therefore, increasing export efficiency resulted in higher proportional amounts of POC and PON in the sediment traps. Increasing the POC

and PON percentages was probably not caused by the rise in the riverine discharge as more terrestrial organic matter would lead to a higher POC/PON ratio, which did not happen. Lui et al. [26] reported that the increasing POC percentage occurred only briefly from 2008 to 2016. The POC flux [42] seems to have declined between 1992 and 1999. Multi-decadal data are necessary to identify any genuine long-term trend. Ground-truth validation is also necessary, as Shih et al. [61] pointed out that in situ productivity measurements are only half of the satellite-derived data in the SCS.

4. Secchi Disk Depth

The SDD reflects the attenuation of light and is a good measure of water transparency or water clarity. SDDs are easy to measure and have been observed for over a century [31,62–64]. The following analyses used the ESA's Globcolour project satellite ocean-derived data with a spatial resolution of 4 km (http://globcolor.info/; accessed in 15 April 2019). Monthly L3m data were used, and trends were assessed pixel by pixel and reported as % change per year. Cloud- and ice-covered areas were masked. See Bai et al. [11] and Chen et al. [14–16] for details.

Generally, a continental shelf, especially in bays, coastal areas, and areas around giant river mouths, is associated with a low SDD because the sediment content and phytoplankton biomass in these areas exceed those in the deeper waters. Notably, rivers export both nutrients and suspended particles. In coastal seas, winds, tidal motion, and shipping and fishing activities disturb sediments beneath and move nutrient-rich bottom waters to the surface layer. Consequently, PP is enhanced by rising chlorophyll content while water clarity falls, lowering SDD. In the deep basins of all three seas, away from landmasses, the SDD is high, but the chlorophyll content is low [14–16]. The seasonal variability of the SDDs in the Bering and Okhotsk Seas, high in winter but low during the warm phytoplankton growing season (Figure 6a,b), is also a mirror image of that of the chlorophyll content (Figure 5a,b). However, the temporal variations of these variables in the SCS are different. Note that when taking averages for a sea, the heavily weighted high-chlorophyll area has a low weight for SDD [14]. As a result, some inconsistencies between the SDD and chlorophyll may arise.

In the SW Bering Sea Basin and off SW Alaska, a marked 2–3%/yr decrease in SDD occurred (blue in Figure 7a), possibly owing to increased chlorophyll concentration (brown in Figure 4a). However, the continental slope and the northern part of the Bering Sea Basin showed increased SDD between 1998 and 2018. On average, despite little change in chlorophyll content in the Bering Sea, a rise in SDD or more transparent water (0.43 m/decade, p = 0.37; Figure 6a) was exhibited. Note that we observed only satellites' near-surface signals, and the subsurface signals may differ. For instance, Rohan et al. [65] reported more turbid subsurface waters in the Eastern Bering Sea from 2004 to 2018.

From 1998 to 2018, the annual mean SDD in the Okhotsk Sea increased by 0.46 m/decade (p = 0.3; Figure 6b), while it declined substantially at a rate of 2–3%/yr in the central basin (Figure 7b), likely as a result of increasing chlorophyll content (Figure 4b). Patches with increased SDD broadly match those of reduced chlorophyll concentration. He et al. [31] reported a much faster increasing rate of SDD (~0.8 m/decade) between 1997 and 2010.

The SCS revealed a slow increase of SDD of 0.29 m/decade (p = 0.36; Figure 6c; Table 1), implying that the SCS water was becoming clearer. This result is consistent with the notion that tropical and subtropical seas generally exhibit significant increases in SDD and decreases in chlorophyll content [49]. The SCS's SDD fell from 1998 to 2005, then increased from 2005 to 2014 (Figure 6c) before declining again. Nevertheless, many coastal regions' SDD decreased (Figure 7c), particularly off the Indochina coast and in the southern Taiwan Strait, possibly due to increasing anthropogenic nutrient outflow and chlorophyll concentration (Figure 4c). However, the SDD increased off the Pearl River estuary. Wang et al. [66] attributed this to the rising sea level, which causes the upstream movement of the maximum estuarine turbidity zone, directly contributing to increased water transparency offshore. He et al. [31] found decreased SDD in the SCS of around

0.8 m/decade from 1998 to 2010. The temporal variation of the SDD from 1998 to 2018 (Figure 6c) reveals that it fell from 1998 to about 2008—consistent with He et al.'s [31] findings—and increased after that.

Further, Bai et al. [11] reported that all 12 of the Eurasian continent's marginal seas they studied exhibited increasing SDD from 2003 to 2014. The Persian Gulf saw the highest percentage increase (3.02%/yr, or 2.5 m/decade). The Java-Banda and the Arabian Seas also increased by around 1.3%/yr or 3.5 m/decade ($p < 0.007$). The other nine marginal seas exhibited growth rates of under 1%/yr. Note that different data coverage and satellite records make meaningful comparisons difficult. For example, Bai et al. [11] started their study in 2003—a year of relatively low SDD, particularly in the SCS (Figure 6c). They ended their analyses in 2014, after which the SDD declined steadily in the Bering and the South China Seas. Limiting the analysis to 2003–2014 would yield a faster increase in SDD. He et al. [31] and Bai et al. [11] used single satellite records from SeaWiFS and Aqua/MODIS, respectively. In contrast, we merged records from multiple satellites [14–16]. Nevertheless, the conclusion based on all records is that the SDD in the Okhotsk Sea increased over the last two decades.

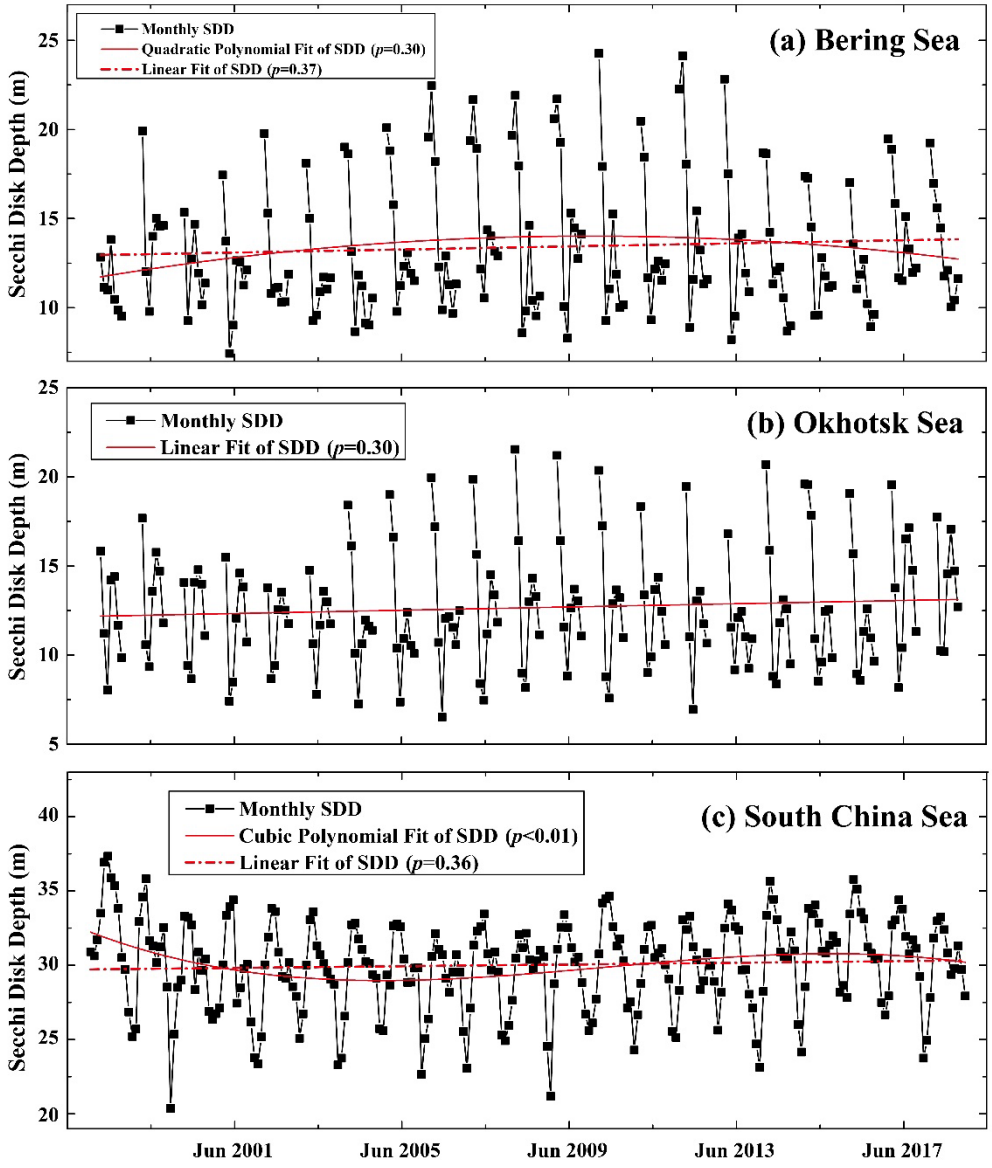

Figure 6. Time series of SDD in the (**a**) Bering, (**b**) Okhotsk, and (**c**) South China Seas during 1998–2018.

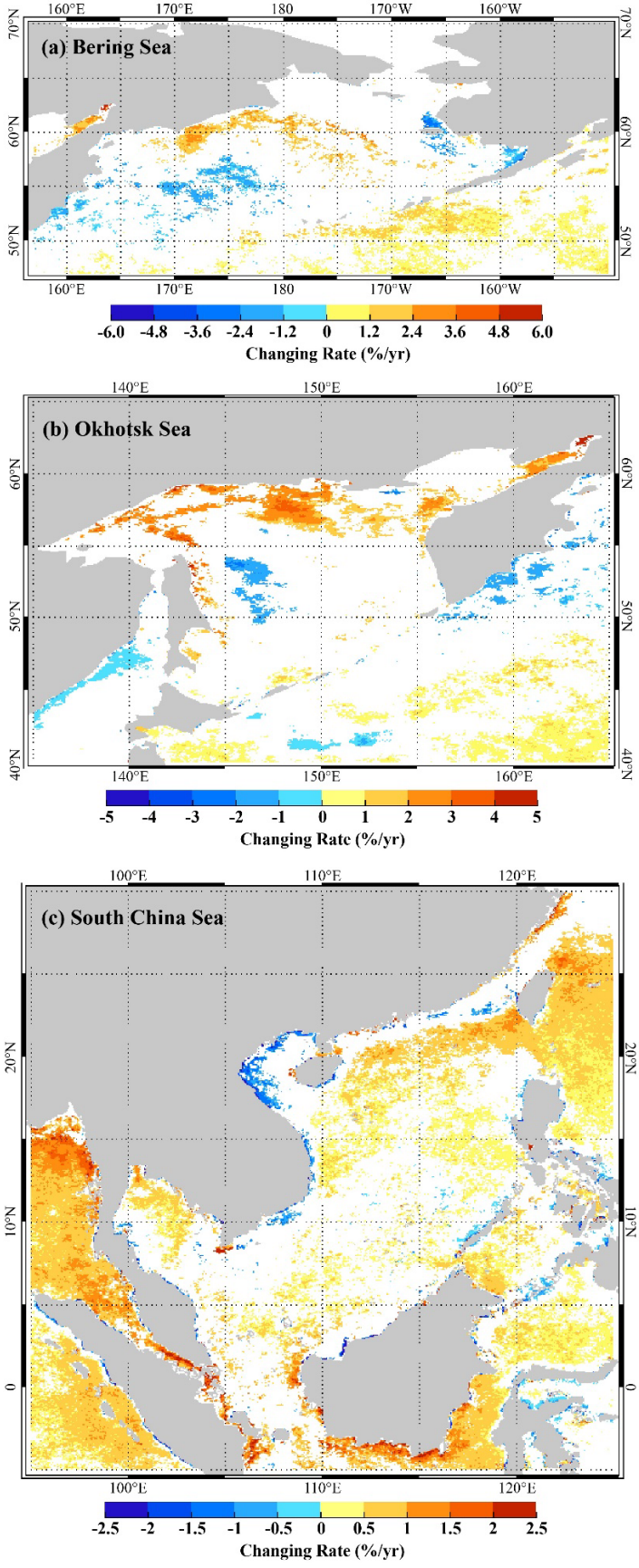

Figure 7. Trend maps of SDD in the (**a**) Bering, (**b**) Okhotsk, and (**c**) South China Seas during 1998–2018 (Bright colors show pixels with $p < 0.1$).

5. Conclusions

This work used satellite-derived time-series records to demonstrate long-term variations in the SST, chlorophyll content, and SDD in the Bering, Okhotsk, and South China Seas from 1998 to 2018. Overall, the SST and the SDD increased by 0.62 °C/decade (p = 0.06) and 0.43 m/decade (p = 0.37), respectively, in the Bering Sea, although the chlorophyll concentrations did not change. In the Okhotsk Sea, the SST, chlorophyll content, and SDD increased by 0.41 °C/decade, 0.047 μg/L/decade, and 0.46 m/decade, respectively. These changes may have altered the seas' biophysical processes and carbon sequestration. For example, oceanic warming has increased chlorophyll concentrations in the Okhotsk Sea, contrary to the established notion that a higher SST leads to lower chlorophyll content in tropical and subtropical oceans.

From 1998 to 2018, the SST in the SCS increased by 0.089 °C/decade, much lower than that in high-latitude oceans. The chlorophyll concentration did not change, but the SDD increased in the SCS by 0.29 m/decade. However, the SST, chlorophyll content, and SDD in the SCS changed in opposite directions in the two periods between 1998–2006 and between 2007–2018. The SST and SDD fell, while the chlorophyll content increased, in the former period. In contrast, the SST and SDD increased, while the chlorophyll content decreased, in the latter period.

All the above changes might have altered the biogeochemical processes in the three seas of interest and possibly in other marginal seas; these possible effects warrant further study. A longer record will also make the trends more meaningful.

Author Contributions: C.-T.C. was responsible for the writing of the manuscript. S.Y., Y.B. and X.H. were responsible for synthesizing the satellite data. T.-H.H. and H.-K.L. helped in writing portions of the manuscript. All authors have read and agreed to the published version of the manuscript.

Funding: This research was partially funded by the Ministry of Science and Technology of Taiwan, MOST 109-2611-M-110-016, and Taiwan's Ministry of Education (Higher Education Sprout Program 11C 0902). China's National Key Research and Development Program (Grant #2017YFA0603003) and the National Natural Science Foundation of China (Grant #41676172) also supported this research.

Data Availability Statement: Not applicable.

Acknowledgments: The authors would like to thank the Ministry of Science and Technology of Taiwan for supporting this research under contract MOST 109-2611-M-110-016 and the Ministry of Education (Higher Education Sprout Program) of Taiwan. China's National Key Research and Development Program (Grant #2017YFA0603003) and the National Natural Science Foundation of China (Grant #41676172) also supported this research. Three anonymous reviewers provided constructive comments.

Conflicts of Interest: The authors declare no conflict of interest.

References

1. Bindoff, N.L.; Cheung, W.W.; Kairo, J.G.; Arístegui, J.; Guinder, V.A.; Hallberg, R.; Hilmi, N.J.M.; Jiao, N.; Karim, M.S.; Levin, L. Changing ocean, marine ecosystems, and dependent communities. In *IPCC Special Report on the Ocean and Cryosphere in a Changing Climate*; IPCC: Geneva, Switzerland, 2019; pp. 477–587.
2. Lotze, H.K.; Tittensor, D.P.; Bryndum-Buchholz, A.; Eddy, T.D.; Cheung, W.W.L.; Galbraith, E.D.; Barange, M.; Barrier, N.; Bianchi, D.; Blanchard, J.L.; et al. Global ensemble projections reveal trophic amplification of ocean biomass declines with climate change. *Proc. Natl. Acad. Sci. USA* **2019**, *116*, 12907–12912. [CrossRef] [PubMed]
3. IPCC. *AR6 Synthesis Report: Climate Change 2022*; IPCC: Geneva, Switzerland, 2022.
4. Chen, C.-T.A.; Huang, T.-H.; Lui, H.-K.; Zhang, J. Unheralded submarine groundwater discharge. *Oceanogr. Fish. Open Access J.* **2019**, *10*, 126–128.
5. Wang, S.L.; Chen, C.T.A.; Huang, T.H.; Tseng, H.C.; Lui, H.K.; Peng, T.R.; Kandasamy, S.; Zhang, J.; Yang, L.Y.; Gao, X.L.; et al. Submarine groundwater discharge helps making nearshore waters heterotrophic. *Sci. Rep.* **2018**, *8*, 11650. [CrossRef] [PubMed]
6. Lui, H.K.; Chen, C.T.A.; Hou, W.P.; Yu, S.J.; Chan, J.W.; Bai, Y.; He, X.Q. Transient carbonate chemistry in the expanded Kuroshio region. In *Changing Asia-Pacific Marginal Seas*; Chen, C.T.A., Guo, X.Y., Eds.; Springer: Singapore, 2020; pp. 307–320. [CrossRef]
7. Chen, C.T.A.; Andreev, A.; Kim, K.R.; Yamamoto, M. Roles of continental shelves and marginal seas in the biogeochemical cycles of the North Pacific Ocean. *J. Oceanogr.* **2004**, *60*, 17–44. [CrossRef]
8. Wiese, F.K.; Van Pelt, T.I.; Wiseman, W.J. Bering Sea linkages. *Deep-Sea Res. Part II* **2012**, *65-70*, 2–5. [CrossRef]

9. Xie, L.L.; Guan, Y.; Hu, J.Y.; Zheng, Q.A. Advances in interscale and interdisciplinary approaches to the South China Sea. *Acta Oceanol. Sin.* **2021**, *40*, 196–199. [CrossRef]
10. Hallett, C.S.; Hobday, A.J.; Tweedley, J.R.; Thompson, P.A.; McMahon, K.; Valesini, F.J. Observed and predicted impacts of climate change on the estuaries of south-western Australia, a Mediterranean climate region. *Reg. Environ. Chang.* **2018**, *18*, 1357–1373. [CrossRef]
11. Bai, Y.; He, X.Q.; Yu, S.J.; Chen, C.T.A. Changes in the Ecological Environment of the Marginal Seas along the Eurasian Continent from 2003 to 2014. *Sustainability* **2018**, *10*, 635. [CrossRef]
12. Stabeno, P.J.; Kachel, N.B.; Moore, S.E.; Napp, J.M.; Sigler, M.; Yamaguchi, A.; Zerbini, A.N. Comparison of warm and cold years on the southeastern Bering Sea shelf and some implications for the ecosystem. *Deep-Sea Res. Part II* **2012**, *65-70*, 31–45. [CrossRef]
13. Wang, M.Y.; Overland, J.E.; Stabeno, P. Future climate of the Bering and Chukchi Seas projected by global climate models. *Deep-Sea Res. Part II* **2012**, *65–70*, 46–57. [CrossRef]
14. Chen, C.T.A.; Yu, S.J.; Huang, T.H.; Bai, Y.; He, X.Q. Changes in temperature, chlorophyll concentration, and Secchi Disk Depth in the Bering Sea from 1998 to 2016. In *Changing Asia-Pacific Marginal Seas*; Chen, C.T.A., Guo, X.Y., Eds.; Springer: Singapore, 2020; pp. 5–18. [CrossRef]
15. Chen, C.T.A.; Yu, S.J.; Huang, T.H.; Bai, Y.; He, X.Q. Changes in temperature, chlorophyll concentration, and Secchi Disk Depth in the Okhotsk Sea from 1998 to 2016. In *Changing Asia-Pacific Marginal Seas*; Chen, C.T.A., Guo, X.Y., Eds.; Springer: Singapore, 2020; pp. 57–68. [CrossRef]
16. Chen, C.T.A.; Yu, S.J.; Huang, T.H.; Lui, H.K.; Bai, Y.; He, X.Q. Changing biogeochemistry in the South China Sea. In *Changing Asia-Pacific Marginal Seas*; Chen, C.T.A., Guo, X.Y., Eds.; Springer: Singapore, 2020; pp. 203–216. [CrossRef]
17. Nakanowatari, T.; Mitsudera, H. Long-term trend and interannual to decadal variability in the Sea of Okhotsk. In *Changing Asia-Pacific Marginal Seas*; Chen, C.T.A., Guo, X.Y., Eds.; Springer: Singapore, 2020; pp. 19–56. [CrossRef]
18. Schmidtko, S.; Stramma, L.; Visbeck, M. Decline in global oceanic oxygen content during the past five decades. *Nature* **2017**, *542*, 335–339. [CrossRef] [PubMed]
19. Breitburg, D.; Levin, L.A.; Oschlies, A.; Grégoire, M.; Chavez, F.P.; Conley, D.J.; Garçon, V.; Gilbert, D.; Gutiérrez, D.; Isensee, K.; et al. Declining oxygen in the global ocean and coastal waters. *Science* **2018**, *359*, eaam7240. [CrossRef] [PubMed]
20. Oschlies, A. A committed fourfold increase in ocean oxygen loss. *Nat. Commun.* **2021**, *12*, 2037. [CrossRef] [PubMed]
21. Qi, D.; Ouyang, Z.; Chen, L.; Wu, Y.; Lei, R.; Chen, B.; Feely, R.A.; Anderson, L.G.; Zhong, W.; Lin, H.; et al. Climate change drives rapid decadal acidification in the Arctic Ocean from 1994 to 2020. *Science* **2022**, *377*, 1544–1550. [CrossRef]
22. Nan, F.; Yu, F.; Xue, H.J.; Zeng, L.L.; Wang, D.X.; Yang, S.L.; Nguyen, K.C. Freshening of the upper ocean in the South China Sea since the early 1990s. *Deep-Sea Res. Part I* **2016**, *118*, 20–29. [CrossRef]
23. Durack, P.J.; Wijffels, S.E. Fifty-year trends in global ocean salinities and their relationship to broad-scale warming. *J. Clim.* **2010**, *23*, 4342–4362. [CrossRef]
24. Nan, F.; Xue, H.J.; Chai, F.; Wang, D.X.; Yu, F.; Shi, M.C.; Guo, P.F.; Xiu, P. Weakening of the Kuroshio intrusion into the South China Sea over the past two decades. *J. Clim.* **2013**, *26*, 8097–8110. [CrossRef]
25. Nan, F.; Xue, H.J.; Yu, F. Kuroshio intrusion into the South China Sea: A review. *Prog. Oceanogr.* **2015**, *137*, 314–333. [CrossRef]
26. Lui, H.K.; Chen, K.Y.; Chen, C.T.A.; Wang, B.S.; Lin, H.L.; Ho, S.H.; Tseng, C.J.; Yang, Y.; Chan, J.W. Physical forcing-driven productivity and sediment flux to the deep basin of Northern South China Sea: A decadal time series study. *Sustainability* **2018**, *10*, 971. [CrossRef]
27. Huang, T.H.; Chen, C.T.A.; Lee, J.; Wu, C.R.; Wang, Y.L.; Bai, Y.; He, X.Q.; Wang, S.L.; Kandasamy, S.; Lou, J.Y.; et al. East China Sea increasingly gains limiting nutrient P from South China Sea. *Sci. Rep.* **2019**, *9*, 5648. [CrossRef]
28. Liu, Y.; Peng, Z.C.; Zhou, R.J.; Song, S.H.; Liu, W.G.; You, C.F.; Lin, Y.P.; Yu, K.F.; Wu, C.C.; Wei, G.J.; et al. Acceleration of modern acidification in the South China Sea driven by anthropogenic CO_2. *Sci. Rep.* **2014**, *4*, 5148. [CrossRef] [PubMed]
29. Lui, H.K.; Chen, C.T.A. Deducing acidification rates based on short-term time series. *Sci. Rep.* **2015**, *5*, 11517. [CrossRef] [PubMed]
30. Screen, J.A.; Simmonds, I. The central role of diminishing sea ice in recent Arctic temperature amplification. *Nature* **2010**, *464*, 1334–1337. [CrossRef] [PubMed]
31. He, X.Q.; Pan, D.L.; Bai, Y.; Wang, T.Y.; Chen, C.T.A.; Zhu, Q.K.; Hao, Z.Z.; Gong, F. Recent changes of global ocean transparency observed by SeaWiFS. *Cont. Shelf Res.* **2017**, *143*, 159–166. [CrossRef]
32. Belkin, I.M. Rapid warming of large marine ecosystems. *Prog. Oceanogr.* **2009**, *81*, 207–213. [CrossRef]
33. IPCC. *Global Warming of 1.5 °C*; IPCC: Geneva, Switzerland, 2018.
34. Wang, M.Y.; Overland, J.E. A sea ice free summer Arctic within 30 years? *Geophys. Res. Lett.* **2009**, *36*, L07502. [CrossRef]
35. Chen, C.T.A. Rare northward flow in the Taiwan Strait in winter: A note. *Cont. Shelf Res.* **2003**, *23*, 387–391. [CrossRef]
36. Naik, H.; Chen, C.T.A. Biogeochemical cycling in the Taiwan Strait. *Estuar. Coast. Shelf Sci.* **2008**, *78*, 603–612. [CrossRef]
37. Han, A.Q.; Dai, M.H.; Gan, J.P.; Kao, S.J.; Zhao, X.Z.; Jan, S.; Li, Q.; Lin, H.; Chen, C.T.A.; Wang, L.; et al. Inter-shelf nutrient transport from the East China Sea as a major nutrient source supporting winter primary production on the northeast South China Sea shelf. *Biogeosciences* **2013**, *10*, 8159–8170. [CrossRef]
38. Chen, C.T.A.; Bai, Y.; Huang, T.H.; He, X.Q.; Chen, H.W.; Yu, S.J. Southward spreading of the Changjiang Diluted Water in the La Nina spring of 2008. *Sci. Rep.* **2021**, *11*, ARTN 307. [CrossRef] [PubMed]

39. Jan, S.; Chen, C.T.A. Potential biogeochemical effects from vigorous internal tides generated in Luzon Strait: A case study at the southernmost coast of Taiwan. *J. Geophys. Res.-Oceans* **2009**, *114*, C04021. [CrossRef]
40. Hsu, P.C.; Lee, H.J.; Zheng, Q.A.; Lai, J.W.; Su, F.C.; Ho, C.R. Tide-induced periodic sea surface temperature drops in the coral reef area of Nanwan Bay, Southern Taiwan. *J. Geophys. Res.-Oceans* **2020**, *125*, ARTN e2019JC015226. [CrossRef]
41. Wu, C.R.; Chang, C.W.J. Interannual variability of the South China Sea in a data assimilation model. *Geophys. Res. Lett.* **2005**, *32*, L17611. [CrossRef]
42. Li, H.L.; Wiesner, M.G.; Chen, J.F.; Ling, Z.; Zhang, J.J.; Ran, L.H. Long-term variation of mesopelagic biogenic flux in the central South China Sea: Impact of monsoonal seasonality and mesoscale eddy. *Deep-Sea Res. Part I* **2017**, *126*, 62–72. [CrossRef]
43. Xu, Z.H.; Ji, F.; Liu, B.; Feng, T.C.; Gao, Y.; He, Y.L.; Chang, F. Long-term evolution of global sea surface temperature trend. *Int. J. Climatol.* **2021**, *41*, 4494–4508. [CrossRef]
44. Giuliani, S.; Bellucci, L.G.; Nhon, D.H. The coast of Vietnam: Present status and future challenges for sustainable development. In *World Seas: An Environmental Evaluation*; Elsevier: Amsterdam, The Netherlands, 2019; pp. 415–435.
45. Chen, C.T.A. Buoyancy leads to high productivity of the Changjiang diluted water: A note. *Acta Oceanol. Sin.* **2008**, *27*, 133–140.
46. Chen, C.T.A.; Wang, S.L.; Lu, X.X.; Zhang, S.R.; Lui, H.K.; Tseng, H.C.; Wang, B.J.; Huang, H.I. Hydrogeochemistry and greenhouse gases of the Pearl River, its estuary and beyond. *Quat. Int.* **2008**, *186*, 79–90. [CrossRef]
47. Dai, M.H.; Lu, Z.M.; Zhai, W.D.; Chen, B.S.; Cao, Z.M.; Zhou, K.B.; Cai, W.J.; Chen, C.T.A. Diurnal variations of surface seawater pCO2 in contrasting coastal environments. *Limnol. Oceanogr.* **2009**, *54*, 735–745. [CrossRef]
48. Walvoord, M.A.; Striegl, R.G. Increased groundwater to stream discharge from permafrost thawing in the Yukon River basin: Potential impacts on lateral export of carbon and nitrogen. *Geophys. Res. Lett.* **2007**, *34*, L12402. [CrossRef]
49. Siegel, D.A.; Behrenfeld, M.; Maritorena, S.; McClain, C.R.; Antoine, D.; Bailey, S.W.; Bontempi, P.S.; Boss, E.S.; Dierssen, H.M.; Doney, S.C.; et al. Regional to global assessments of phytoplankton dynamics from the SeaWiFS mission. *Remote Sens. Environ.* **2013**, *135*, 77–91. [CrossRef]
50. Giesbrecht, K.; Varela, D.; Wiktor, J.; Grebmeier, J.; Kelly, B.; Long, J. A decade of summertime measurements of phytoplankton biomass, productivity and assemblage composition in the Pacific Arctic Region from 2006 to 2016. *Deep-Sea Res. Part II* **2019**, *162*, 93–113. [CrossRef]
51. Thomas, M.K.; Kremer, C.T.; Klausmeier, C.A.; Litchman, E. A global pattern of thermal adaptation in marine phytoplankton. *Science* **2012**, *338*, 1085–1088. [CrossRef] [PubMed]
52. Wohlers, J.; Engel, A.; Llner, E.; Breithaupt, P.; Rgens, K.; Hoppe, H.-G.; Sommer, U.; Riebesell, U. Changes in biogenic carbon flow in response to sea surface warming. *Proc. Natl. Acad. Sci. USA* **2009**, *106*, 7067–7072. [CrossRef] [PubMed]
53. Yu, Y.; Xing, X.G.; Liu, H.L.; Yuan, Y.P.; Wang, Y.T.; Chai, F. The variability of chlorophyll-a and its relationship with dynamic factors in the basin of the South China Sea. *J. Marine Syst.* **2019**, *200*, ARTN 103230. [CrossRef]
54. Lui, H.-K.; Chen, C.-T.A.; Hou, W.-P.; Liau, J.-M.; Chou, W.-C.; Wang, Y.-L.; Wu, C.-R.; Lee, J.; Hsin, Y.-C.; Choi, Y.-Y. Intrusion of Kuroshio helps to diminish coastal hypoxia in the coast of northern South China Sea. *Front. Mar. Sci.* **2020**, *7*, 565952. [CrossRef]
55. Palacz, A.P.; Xue, H.J.; Armbrecht, C.; Zhang, C.Y.; Chai, F. Seasonal and inter-annual changes in the surface chlorophyll of the South China Sea. *J. Geophys. Res.-Oceans* **2011**, *116*, C09015. [CrossRef]
56. Li, Q.P.; Wang, Y.J.; Dong, Y.; Gan, J.P. Modeling long-term change of planktonic ecosystems in the northern South China Sea and the upstream Kuroshio Current. *J. Geophys. Res.-Oceans* **2015**, *120*, 3913–3936. [CrossRef]
57. Gregg, W.W.; Rousseaux, C.S. Global ocean primary production trends in the modern ocean color satellite record (1998–2015). *Environ. Res. Lett.* **2019**, *14*, ARTN 124011. [CrossRef]
58. Li, T.; Bai, Y.; He, X.Q.; Tao, B.Y.; Chen, X.Y.; Gong, F.; Wang, T.Y. Phytoplankton size classes changed oppositely over shelf and basin areas of the South China Sea during 2003–2018. *Prog. Oceanogr.* **2021**, *191*, ARTN 102496. [CrossRef]
59. Li, T.; Bai, Y.; He, X.Q.; Chen, X.Y.; Chen, C.T.A.; Tao, B.Y.; Pan, D.L.; Zhang, X. The relationship between POC export efficiency and primary production: Opposite on the shelf and basin of the northern South China Sea. *Sustainability* **2018**, *10*, 3634. [CrossRef]
60. Chen, Y.L.L. Spatial and seasonal variations of nitrate-based new production and primary production in the South China Sea. *Deep-Sea Res. Part I* **2005**, *52*, 319–340. [CrossRef]
61. Shih, Y.Y.; Shiah, F.K.; Lai, C.C.; Chou, W.C.; Tai, J.H.; Wu, Y.S.; Lai, C.Y.; Ko, C.Y.; Hung, C.C. Comparison of primary production using in situ and satellite-derived values at the SEATS Station in the South China Sea. *Front. Mar. Sci.* **2021**, *8*, ARTN 747763. [CrossRef]
62. He, X.Q.; Bai, Y.; Pan, D.L.; Huang, N.L.; Dong, X.; Chen, J.S.; Chen, C.T.A.; Cui, Q.F. Using geostationary satellite ocean color data to map the diurnal dynamics of suspended particulate matter in coastal waters. *Remote Sens. Environ.* **2013**, *133*, 225–239. [CrossRef]
63. He, X.; Bai, Y.; Pan, D.; Chen, C.T.A.; Cheng, Q.; Wang, D.; Gong, F. Satellite views of the seasonal and interannual variability of phytoplankton blooms in the eastern China seas over the past 14 yr (1998–2011). *Biogeosciences* **2013**, *10*, 4721–4739. [CrossRef]
64. He, X.Q.; Bai, Y.; Chen, C.T.A.; Hsin, Y.C.; Wu, C.R.; Zhai, W.D.; Liu, Z.L.; Gong, F. Satellite views of the episodic terrestrial material transport to the southern Okinawa Trough driven by typhoon. *J. Geophys. Res.-Oceans* **2014**, *119*, 4490–4504. [CrossRef]

65. Rohan, S.K.; Kotwicki, S.; Kearney, K.A.; Schulien, J.A.; Laman, E.A.; Cokelet, E.D.; Beauchamp, D.A.; Britt, L.L.; Aydin, K.Y.; Zador, S.G. Using bottom trawls to monitor subsurface water clarity in marine ecosystems. *Prog. Oceanogr.* **2021**, *194*, ARTN 102554. [CrossRef]
66. Wang, J.; Tong, Y.; Feng, L.; Zhao, D.; Zheng, C.M.; Tang, J. Satellite-observed decreases in water turbidity in the Pearl River Estuary: Potential linkage with sea-level rise. *J. Geophys. Res.-Oceans* **2021**, *126*, ARTN e2020JC016842. [CrossRef]